


 Cite this: *RSC Adv.*, 2020, 10, 95

Controlled release of basic fibroblast growth factor from a water-floatable polyethylene nonwoven fabric sheet for maintenance culture of iPSCs

 Ayako Oyane,^a Hiroko Araki,^a Maki Nakamura,^a Yasuhiko Aiki,^b Kumiko Higuchi,^b Alexander Pyatenko,^c Masaki Adachi^d and Yuzuru Ito^b

Basic fibroblast growth factor (bFGF) is an essential supplement for culture media to support the proliferation of human pluripotent stem cells, while preserving their pluripotency. However, it is extremely unstable under cell culture conditions at 37 °C. Therefore, a culture medium supplemented with bFGF needs to be changed every day to maintain an effective concentration of bFGF. This study aimed to create a bFGF-releasing material via simple bFGF adsorption following oxygen plasma treatment by using a water-floatable polyethylene (PE) nonwoven fabric sheet as a bFGF-adsorbent material. Preliminary oxygen plasma treatment enhanced bFGF adsorption onto the sheet by increasing its surface water wettability. Based on the bFGF concentration in the adsorption solution, the resulting bFGF-adsorbed sheet showed different bFGF-release profiles in the culture medium. The bFGF-adsorbed sheet prepared under optimum conditions released bFGF in a sustained manner, maintaining the bFGF concentration in the culture medium of human induced pluripotent stem cells (iPSCs) at ≥ 10 ng mL⁻¹ even without medium change for as long as 3 d. The bFGF released from the sheet retained its biological activity to support colony formation of iPSCs while preserving their pluripotency. This type of bFGF-releasing sheet can be used as a new form of bFGF supplement for the culture media of stem cells and would make a significant contribution to stem cell-based research and development.

 Received 30th August 2019
Accepted 13th December 2019

DOI: 10.1039/c9ra06906b

rsc.li/rsc-advances

1 Introduction

Basic fibroblast growth factor (bFGF) is a signaling protein that controls the migration, proliferation, differentiation, and survival of various cell types.¹ bFGF is also involved in a wide range of biological processes, such as angiogenesis,² hematopoiesis,³ and tissue/organ repair and regeneration.^{4–6} bFGF plays an important role in supporting the proliferation of human pluripotent stem cells, such as induced pluripotent stem cells (iPSCs) and embryonic stem cells, while retaining their pluripotency.^{7–10} In maintenance cultures of human stem cells, recombinant bFGF (around 10 ng mL⁻¹) is used as a culture medium supplement to prevent spontaneous differentiation of stem cells.^{10,11} However, bFGF is extremely unstable under cell culture conditions at 37 °C;^{12–14} it loses most of its

biological activity (extracellular receptor kinase phosphorylation) within 24 h at 37 °C because of molecular aggregation.¹² Hence, frequent medium change (typically once a day) is indispensable to maintain an effective concentration of bFGF in the culture medium and to preserve the pluripotency of stem cells. This has been one of the most critical factors increasing material and labor costs in stem cell-based research and development.

Recently, a new bFGF supplement for stem cell culture was developed: bFGF-immobilized biodegradable poly(lactic-co-glycolic acid) microbeads.¹⁴ These microbeads maintain constant bFGF concentration in the medium (8–10 ng mL⁻¹) by releasing bFGF, thereby reducing the frequency of medium change required for stem cell maintenance to twice a week. Despite such advantages, the microbeads pose a concern with respect to their physical effects on cells. That is, they sink in the medium to come into contact with cellular surfaces, unless a culture plate insert is employed. More recently, a film-type bFGF supplement for stem cell culture was developed: multi-layered nanofilm composed of a repeating polycation/polyanion/bFGF structure.¹⁵ This nanofilm, inserted into a culture plate, delivers bFGF to the cells in a non-contact manner even without the use of a culture plate insert. However, both of the above bFGF supplements may release not only bFGF but also heparin and degradation products of their

^aNanomaterials Research Institute, National Institute of Advanced Industrial Science and Technology (AIST), Central 5, 1-1-1 Higashi, Tsukuba, Ibaraki 305-8565, Japan. E-mail: a-oyane@aist.go.jp

^bBiotechnology Research Institute for Drug Discovery, National Institute of Advanced Industrial Science and Technology (AIST), Central 6, 1-1-1 Higashi, Tsukuba, Ibaraki 305-8566, Japan

^cNational Institute of Advanced Industrial Science and Technology (AIST), Central 5, 1-1-1 Higashi, Tsukuba, Ibaraki 305-8565, Japan

^dR&D Center, Katayama Chemical Industries Co., Ltd., 4-1-7 Ina, Minoh, Osaka 562-0015, Japan



matrixes. Heparin is contained in these bFGF supplements as a binding and stabilizing agent of bFGF, although it can react with a number of other biomolecules and affect cells. There are many other bFGF-releasing materials consisting of degradable matrixes, such as ester- or ether-based polymers,^{16–18} polysaccharides,^{19,20} polypeptide- or protein-based materials,^{21–24} and low-crystalline calcium phosphates.^{25,26} However, all result in the formation of degradation products, which alter the medium conditions. For instance, low-crystalline apatite increases Ca and P concentrations in an aqueous medium *via* degradation.²⁷

This study aimed to create a new form of bFGF-releasing material that can be used as a bFGF supplement for stem cell culture. To address the concern about physical effects, we used a water-floatable material for bFGF immobilization. In a normal adherent culture system of stem cells, a water-floatable material is distant from the cells and hence, delivers bFGF to the cells in a non-contact manner even without the aid of a culture plate insert. To address the concern regarding biological effects, we immobilized bFGF on the water-floatable material by simple adsorption without using either bFGF-binding agents or degradable matrixes. We selected a nonwoven fabric sheet composed of polyethylene (PE) microfibers as a water-floatable bFGF adsorbent because it is lighter than water, is chemically stable (nondegradable), and has a large surface area. This water-floatable PE nonwoven fabric sheet is air- and moisture-permeable because of its interconnected nanoporous structure and has been commercialized as paper for sterilization bags.

The as-received PE nonwoven fabric sheet had a hydrophobic and water-repulsive surface; therefore, we first treated it with oxygen plasma to increase its water wettability. We assessed the adsorption and release of bFGF using untreated and oxygen plasma-treated sheets by enzyme-linked immunosorbent assay (ELISA). Subsequently, we systematically varied bFGF adsorption conditions to obtain a bFGF-releasing sheet with the ability to maintain the bFGF concentration of ≥ 10 ng mL⁻¹ in the culture medium for as long as 3 d. The thus-prepared sheet was used to demonstrate the function to support colony formation of human iPSCs, while retaining their pluripotency, in a medium-change-free continuous culture for 3 d.

2 Materials and methods

2.1 Preparation of nonwoven fabric sheets

We used a 180 μ m-thick water-floatable PE nonwoven fabric sheet (Tyvek® 1073B; DuPont, USA) generously supplied by DuPont-Asahi Flash Spun Products Co., Ltd., Japan. The sheet comprises 100% high-density PE microfibers with a diameter of 0.5–10 μ m (average diameter of 4 μ m), randomly oriented and bound to one another by thermal pressing. Additionally, the sheet is air- and moisture-permeable and has a basis weight of 74.6 g m⁻² (range: 71.2–78.0 g m⁻²) and a Gurley–Hill porosity of 22 s/100 cm³ (range: 8–36 s/100 cm³) according to the manufacturer's product information sheet.

The as-received PE nonwoven fabric sheet was cut into 10 mm \times 10 mm using a lever-controlled sample cutter (SDL-

200; DUMBBELL Co., Ltd., Japan), ultrasonically washed with ultrapure water and ethanol, dried in air, and stored in a desiccator before further use. The thus-prepared sheet pieces are hereafter referred to as P00 sheets.

2.2 Oxygen plasma treatment

Some of the P00 sheets were subjected to oxygen plasma treatment; one surface of the P00 sheets was treated using a compact ion etcher (Model FA-1, Samco International Inc., Japan). Oxygen plasma treatment was conducted for 30 s in oxygen gas at a pressure of 30 Pa under an electric field operating at 13.56 MHz. The plasma power density was adjusted to 0.05, 0.10, or 0.20 W cm⁻², and the oxygen plasma-treated sheets were denoted as P05, P10, and P20, respectively.

A colored aqueous solution was prepared by dissolving red food coloring (85% dextrin and 15% new coccine dye; Kyoritsu Foods Co., Ltd., Japan) in phosphate-buffered saline (PBS) (D-PBS(-); FUJIFILM Wako Pure Chemical Corporation, Japan). To examine the effect of oxygen plasma treatment on the floating state of the sheets in aqueous solution, the P00 and P10 sheets were placed over the colored aqueous solution, and their images were captured using a digital camera (Tough TG-5; Olympus Corporation, Japan).

2.3 bFGF adsorption

bFGF solutions of different concentrations ($x = 0$ –12 μ g mL⁻¹) were prepared by diluting the bFGF source with PBS. The bFGF source was 1 mg mL⁻¹ of human recombinant bFGF (bFGF AF, Katayama Chemical Industries Co., Ltd., Japan) with a theoretical molecular mass of 16 539 and an isoelectric point of 9.58. Next, the P00, P05, P10, and P20 sheets sterilized by exposure to ethylene oxide gas were subjected to bFGF adsorption using the bFGF solutions prepared. Each sheet was immersed (oxygen plasma-treated surface down) in 1 mL of the bFGF solutions in a sealed polystyrene tube at 25 °C for various adsorption periods of up to 48 h under shaking or static conditions. The shaking conditions for acellular experiments were set at 67 rpm with a swing of 3 cm using a shaking incubator (PIC-100S; AS ONE Corporation, Japan) and for cellular experiments at 200 rpm with a rotation diameter of 1 cm using a shaking incubator (DWMMaxM BR-104P; TAITEC CORPORATION, Japan). We confirmed that the bFGF-adsorbed P10 sheets prepared under these two shaking conditions exhibited comparable release profiles of bFGF. After bFGF adsorption, the sheets were removed from the bFGF solutions and washed thrice with ultrapure water before surface analyses (Section 2.5) or PBS before bFGF-release and cellular assays (Sections 2.6, 2.7, and 2.8).

The P10 sheets after 24 h adsorption using the 0, 0.5, 1, 2, 4, 8, and 12 μ g mL⁻¹ bFGF solutions under shaking conditions are denoted as P10F0, P10F0.5, P10F1, P10F2, P10F4, P10F8, and P10F12, respectively.

2.4 Chemical analyses of bFGF solutions

Residual bFGF in the bFGF solutions with the P10 sheet after a specific adsorption period was quantified by ELISA. After

various adsorption periods of up to 48 h, 10 μL aliquots were sampled from the bFGF solutions and frozen at $-80\text{ }^\circ\text{C}$ before ELISA. The as-prepared bFGF solutions were also frozen at $-80\text{ }^\circ\text{C}$ before ELISA. The sampled bFGF solutions were diluted with a serum-free acellular culture medium (Essential 6; Thermo Fisher Scientific, USA) and assayed for bFGF using a human FGF basic Quantikine[®] ELISA kit (R&D Systems, Inc., USA). The Essential 6 medium is a chemically defined basic medium commonly used for stem cell culture (components based on Chen's "E8" medium²⁸), and will be used in the assays in Sections 2.6, 2.7, and 2.8. Standard bFGF solutions were prepared by diluting the bFGF source with the same medium. The bFGF residual rate was determined as a percentage of the residual bFGF concentration (C) in the bFGF solutions for a specific adsorption period among the initial bFGF concentrations (C_0) in the as-prepared bFGF solutions as follows:

$$\text{Residual rate of bFGF [\%]} = 100 \times C/C_0 \quad (1)$$

As a control, the same bFGF solution without the P10 sheet was assayed in the same manner as described above. The amount of bFGF adsorbed onto each sheet was estimated by subtracting the residual bFGF in the bFGF solution from that in the control solution without sheets.

2.5 Surface analyses of the sheets

The surfaces of the sheets were analyzed using a field emission scanning electron microscope (SEM) (S-4800; Hitachi High-Technologies Corp., Japan), a contact angle meter (Drop Master DM500; Kyowa Interface Science Co. Ltd., Japan), an X-ray photoelectron spectrometer (XPS) (AXIS Nova; Kratos Analytical Ltd., UK) with Al $K\alpha$ X-rays, and a Fourier transform infrared spectrometer (FT-IR) (FT/IR-4700; JASCO Corporation, Japan) equipped with an attenuated total reflection accessory with a monolithic diamond crystal. Prior to SEM observation, the sheet surfaces were sputter-coated with gold. In contact angle measurement, the sheets were fixed on a flat plate with adhesive tape to flatten their surfaces. The image of an ultra-pure water droplet was captured immediately after 1 μL of a drop established contact with the sheet surfaces. In XPS measurements, the C_{1s} main peak (C-C) of the sheets was set to the binding energy of 284.6 eV.

2.6 bFGF-release assay in an acellular culture medium

bFGF release from the sheets was assayed using the Essential 6 medium. Following bFGF adsorption (Section 2.3), each sheet was placed (oxygen plasma-treated surface down) over 2 mL of the Essential 6 medium in a 24-well culture plate and kept at $37\text{ }^\circ\text{C}$ in a humidified CO_2 (5%) incubator. After incubation for 1, 2, and 3 d, 150 μL aliquots were sampled from the medium, and same amounts of fresh medium were added to the wells to compensate the medium loss. As a control, the Essential 6 medium supplemented with 10 ng mL^{-1} of bFGF was incubated under the same conditions, and 150 μL aliquots were sampled from the as-prepared medium and that after incubation for 1 d.

The sampled solutions were frozen at $-80\text{ }^\circ\text{C}$ and used for ELISA following the protocol described in Section 2.4.

2.7 bFGF-release assay in an iPSC-containing culture medium

bFGF release from the P10F12 sheet was assayed under the culturing of human iPSCs (cell line 201B7;²⁹ RIKEN BioResource Research Center, Japan). The iPSCs were maintained before use as per a standard protocol, as described earlier.³⁰ We used a 6-well culture plate coated with extracellular matrix proteins (Corning[®] Matrigel[®] Growth Factor Reduced Basement Membrane Matrix; Corning Incorporated, USA). For subculture, the iPSCs were manually dissociated from the plate after treatment with EDTA (Versene[®] (EDTA), 0.02%; Lonza, Switzerland) for 5 min at $37\text{ }^\circ\text{C}$.

The iPSCs were precultured (approximately 1.6×10^5 cells/2 mL per well) for 1 d at $37\text{ }^\circ\text{C}$ in 2 mL of the bFGF-containing medium: the Essential 6 medium supplemented with 2 ng mL^{-1} transforming growth factor beta 1 (TGF- β 1) (R&D Systems) and 10 ng mL^{-1} bFGF. The same medium without bFGF was prepared as a control (referred to as "bFGF-free medium"). After preculturing for 1 d, the bFGF-containing medium was replaced with 2 mL of the bFGF-free medium, and the P10F12 sheet was placed (oxygen plasma-treated surface down) over the medium (Day 0). The iPSCs were then cultured in the presence of the P10F12 sheet for another 3 d without changing the medium. As a positive control, the precultured iPSCs were cultured for another 3 d under conventional conditions: in 2 mL of the bFGF-containing medium with daily change of the medium. As a cell-free control, the P10F12 sheet was placed (oxygen plasma-treated surface down) over 2 mL of the bFGF-free medium without iPSCs and incubated for 3 d under the same conditions, as described above. After incubation for 1 d (Day 1), 2 d (Day 2), and 3 d (Day 3), 10 μL aliquots were sampled from the medium. Medium sampling for the positive control was performed just before daily medium change at Days 1, 2, and 3. The sampled solutions were frozen at $-80\text{ }^\circ\text{C}$ and used for ELISA following the same protocol as described in Section 2.4, except that the medium for sample dilution was changed to that used in this cellular experiment.

2.8 Assay of cultured iPSCs

Colony formation, viability, and pluripotency of the cultured iPSCs were assayed. As described in Section 2.7, the precultured iPSCs were cultured for 3 d in the bFGF-free medium supplemented with the selected P10F12 sheet without medium change (Culture 1). The same culture process was repeated once after subculture (Culture 2). As positive and negative controls, the precultured iPSCs were cultured in 2 mL of the bFGF-containing and bFGF-free media, respectively, with daily medium change.

We observed the iPSCs *in situ* (without removing the sheet) at Day 3 in Cultures 1 and 2 by using a phase contrast microscope (AXIO Vert.A1; Zeiss, Germany). At Day 3 in Culture 1, the total and viable iPSCs in each well were counted using a cell viability analyzer (Vi-CELL XR; Beckman Coulter, Inc., USA) after dissociating them from the plate with a cell detachment solution

(Accutase™; Innovative Cell Technologies, Inc., USA). After Culture 2, the pluripotency of the cultured iPSCs was assessed by lectin (rBC2LCN) and immunofluorescence (Nanog, Oct-3/4) staining, as described earlier.³¹ These three markers have been established as probes for human pluripotent stem cells, including iPSCs.³¹ First, we removed the sheet by tweezers from the medium, fixed the cultured iPSCs with 4% paraformaldehyde for 10–60 min at 4 °C or room temperature, and rinsed the iPSCs with PBS (DPBS, no calcium, no magnesium; Thermo Fisher Scientific). For lectin staining, the fixed iPSCs were incubated at room temperature for 1 h with 10 μg mL⁻¹ of fluorescein isothiocyanate (FITC)-conjugated rBC2LCN (FUJIFILM Wako Pure Chemical Corporation) diluted in PBS (Takara Bio, Inc., Japan) containing 1% bovine serum albumin (BSA). For immunofluorescence staining, the fixed iPSCs were incubated overnight with a primary antibody diluted in 1% BSA and 5% serum-containing PBS (Takara) at 4 °C. The primary antibodies used were anti-Oct-3/4 (1 : 300 dilution, Santa Cruz Biotechnology, Inc., USA) and anti-Nanog (1 : 800 dilution, Cell Signaling Technology, Inc., USA). Secondary staining was performed with an appropriate secondary antibody conjugated with a fluorescence dye (anti-mouse immunoglobulin M-Alexa 488 or anti-mouse IgG-Alexa 488, 1 : 300 dilution; Thermo Fisher Scientific) for 1 h at room temperature. The iPSCs were counterstained with 4',6-diamidino-2-phenylindole (DAPI) (Dojindo Laboratories, Japan). Cellular images were captured using a fluorescence microscope (BIOREVO BZ-9000; Keyence Corporation, Japan).

2.9 Statistical analysis

In contact angle and XPS measurements (Section 2.5), three different regions on the sheet surface were analyzed to obtain the average and standard deviation (SD). In the quantitative assays (Sections 2.4, 2.6, 2.7, and 2.8), three sheets were independently used for each condition to obtain the average and SD. Statistical differences were determined using Student's *t*-test, and *p* < 0.05 was considered statistically significant.

3 Results

3.1 Effect of oxygen plasma treatment on surface chemistry of the sheet

Oxygen plasma treatment increased surface wettability of the PE nonwoven fabric sheet without altering its microstructure. The P00 sheet comprised randomly oriented microfibers (see the top image in Fig. 1a). As shown in Fig. 1a, the P05, P10, and P20 sheets had surface morphologies similar to that of the P00 sheet, suggesting that oxygen plasma treatment did not cause any apparent morphological changes on the sheet surface under the tested power densities of 0.05, 0.10, or 0.20 W cm⁻².

Contact angle of the ultrapure water droplet on the P05, P10, and P20 sheets was 30–40°, which was less than one-third of that (approximately 120°) on the P00 sheet (Fig. 1b). The P05, P10, and P20 sheets showed similar water contact angles, although the contact angle on the P20 sheet was lower than that on the P05 sheet. Fig. 1c shows digital camera (upper) and side-

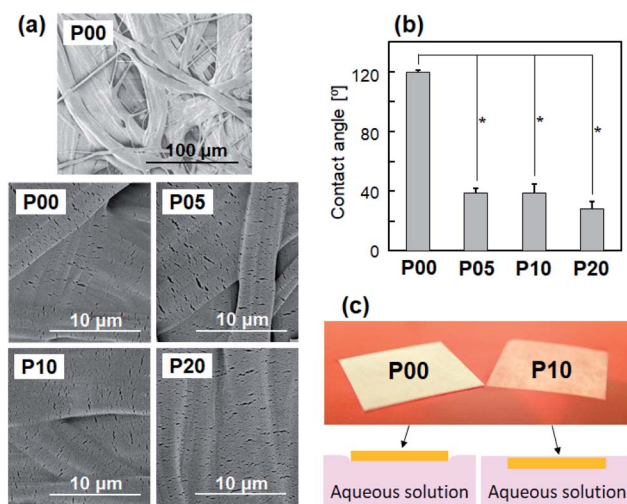


Fig. 1 (a) Lower (upper) and higher (middle, lower) magnification SEM images and (b) contact angles (average + SD; *n* = 3; **p* < 0.05) of an ultrapure water droplet on the surfaces of the P00, P05, P10, and P20 sheets. (c) Digital camera (upper) and side-view schematic (lower) images of the P00 (left) and P10 (right) sheets that were placed over the colored aqueous solution.

view schematic (lower) images of the P00 (left) and P10 (right) sheets placed over a colored aqueous solution. The digital camera images were captured within a few tens of minutes after placing the sheets. As can be observed in the images on the left, the P00 sheet floated on the surface of the solution. In contrast, the P10 sheet floated in the solution (stayed under the surface). These results indicate that oxygen plasma treatment altered the hydrophobic surface of the PE nonwoven fabric sheet to a hydrophilic one with increased water wettability.

The increased water wettability of the plasma-treated sheets is due to plasma-induced surface modification with oxygen-containing polar functional groups. As the P00 sheet comprises pure PE (molecular formula $[-CH_2-CH_2-]_n$), it

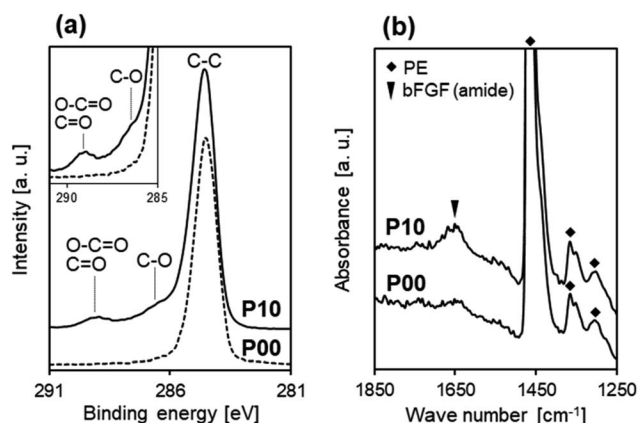


Fig. 2 (a) C_{1s} XPS spectra of the surfaces of the P00 and P10 sheets and (b) FT-IR spectra of their surfaces after 24 h adsorption using the 12 μg mL⁻¹ bFGF solution under shaking conditions. Inset in (a) shows C_{1s} XPS spectra enlarged in the y-axis direction to represent the formation of functional groups.

contains no oxygen before plasma treatment. Fig. 2a shows C_{1s} XPS spectra of the surfaces of the P00 and P10 sheets. In the C_{1s} XPS spectra, a small peak at around 289 eV ascribed to O–C=O and C=O bonds, and a shoulder at around 286.5 eV ascribed to C–O bond³² newly appeared after oxygen plasma treatment (for P10). According to XPS surface compositional analysis, oxygen plasma treatment increased the O/C atomic ratio at the sheet surface from 0.01 ± 0.01 (for P00) to 0.15 ± 0.01 (for P10). These results indicate the formation of oxygen-containing functional groups, such as COOH, CHO, and OH, on the P10 sheet surface, which is in agreement with previous reports.^{33,34}

3.2 Effect of oxygen plasma treatment on bFGF adsorption onto the sheet

bFGF adsorption onto the PE nonwoven fabric sheet was enhanced by the prior plasma treatment. Fig. 2b shows FT-IR spectra of the P00 and P10 sheet surfaces after 24 h bFGF adsorption using the $12 \mu\text{g mL}^{-1}$ bFGF solution under shaking conditions. The reflection peak at 1650 cm^{-1} ascribed to amide groups from bFGF was clearly detected for the P10 sheet, but barely detected for the P00 sheet, suggesting that a larger amount of bFGF adsorbed onto the surface of the P10 sheet than that of the P00 sheet.

3.3 Effect of oxygen plasma treatment on the bFGF-release ability of the sheet

As reported elsewhere, bFGF was highly unstable under the conventional cell culture condition at 37°C . As shown in Fig. 3, free bFGF (10 ng mL^{-1}) added to the acellular culture medium (37°C) became hardly detectable (0.3 ng mL^{-1}) by ELISA within 1 d. Namely, the residual rate of free bFGF after incubation for 1 d was only 3% under the tested condition. This was probably due to the spontaneous conformational change of bFGF molecules in the medium¹² and/or nonspecific bFGF adsorption onto

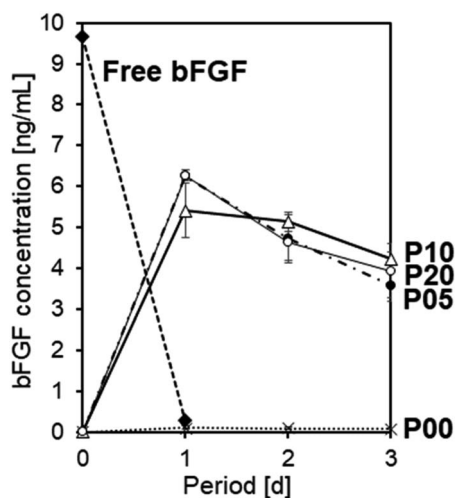


Fig. 3 Release profiles of bFGF in the acellular culture medium from the P00, P05, P10, and P20 sheets after 24 h adsorption using the $4 \mu\text{g mL}^{-1}$ bFGF solution under static conditions (average \pm SD; $n = 3$) compared with the concentration change of free bFGF (initial concentration = 10 ng mL^{-1}) in the culture medium.

the wells' inner wall.³⁵ Note that “bFGF concentration” in this report represents the concentration of ELISA-detectable bFGF, that is, bFGF that retains its binding sites for a monoclonal antibody specific to human bFGF.

The plasma-treated and bFGF-adsorbed sheets released bFGF into the acellular culture medium and retained the bFGF concentration in the medium at a nanogram level for as long as 3 d. The P00, P05, P10, and P20 sheets after 24 h bFGF adsorption using the $4 \mu\text{g mL}^{-1}$ bFGF solution under static conditions were immersed in the acellular medium (37°C) to assess their bFGF-release ability. As shown in Fig. 3, the P05, P10, and P20 sheets released bFGF, thereby retaining a relatively high concentration of bFGF ($3\text{--}7 \text{ ng mL}^{-1}$) in the medium for up to 3 d. In contrast, the P00 sheet hardly raised the bFGF concentration in the medium ($<0.2 \text{ ng mL}^{-1}$), indicating a lack of its bFGF-release ability. These results suggest that the prior plasma treatment is crucial to provide the PE nonwoven fabric sheet with the bFGF-release ability.

Even with any of the plasma-treated sheets (P05, P10, and P20), the bFGF concentration in the culture medium was insufficient for the target level (10 ng mL^{-1}). Thus, to further increase the bFGF-release ability of the sheets, we altered the bFGF adsorption conditions while maintaining the plasma power density constant at 0.1 W cm^{-2} (the condition used for P10) in subsequent experiments. This plasma power density was selected because P10 exhibited the highest bFGF concentration (average value) at 3 d among P05, P10, and P20, although the difference was not statistically significant (Fig. 3).

3.4 Effect of adsorption period and shaking on bFGF adsorption onto the sheet

Shaking the bFGF solution was effective in accelerating bFGF adsorption onto the P10 sheet. The P10 sheet was immersed in the $4 \mu\text{g mL}^{-1}$ bFGF solution under both static and shaking conditions to allow bFGF adsorption onto its surface. At various adsorption periods of up to 48 h, bFGF concentrations of the solutions with and without the P10 sheet were assayed by ELISA.

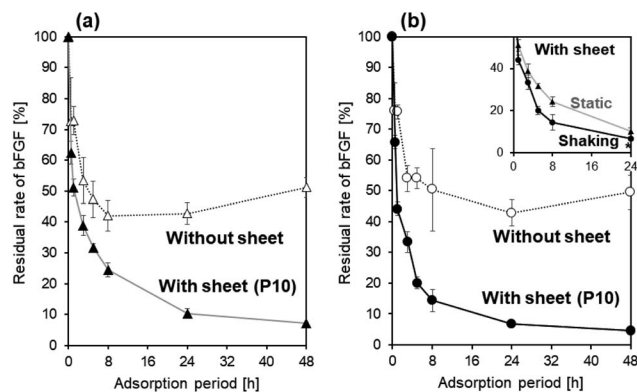


Fig. 4 Variation with bFGF adsorption period of the bFGF residual rate in the $4 \mu\text{g mL}^{-1}$ bFGF solution with and without the P10 sheet under (a) static and (b) shaking conditions (average \pm SD; $n = 3$). Inset in (b) shows a comparison between the static (triangles) and shaking (circles) conditions with the P10 sheet.

The residual rates of bFGF (%) in the bFGF solution were calculated using eqn (1) and plotted as a function of the adsorption period under static (Fig. 4a) and shaking (Fig. 4b) conditions. Even without a P10 sheet in the solution, the bFGF residual rate decreased by approximately half after 8 h under both static and shaking conditions. These results suggest that ELISA-detectable bFGF in the bFGF solution naturally halved within 8 h regardless of the presence of the P10 sheet, probably because of the spontaneous conformational change of bFGF¹² and/or bFGF adsorption onto the tube's inner wall, as described in Section 3.3.³⁵ Under both static and shaking conditions, the bFGF residual rate in the bFGF solution became lower ($p < 0.05$) in the presence of the P10 sheet throughout the bFGF adsorption period from 1 h up to 48 h. This difference between the two solutions with and without the P10 sheet was due to bFGF adsorption onto the P10 sheet surface. When a comparison was made between the static and shaking conditions for the bFGF solution with the P10 sheet (see inset in Fig. 4b), the bFGF residual rate decreased faster under shaking than under static conditions. The shaking condition resulted in the lower ($p < 0.05$) bFGF residual rate than the static condition except for the initial stage within 3 h. Therefore, it can be inferred that bFGF adsorbed onto the P10 sheet surface faster under shaking than under static conditions. Under shaking conditions (see Fig. 4b), the bFGF concentration in the bFGF solution decreased, while the amount of bFGF adsorbed onto the P10 sheet surface increased with increasing adsorption period up to 24 h and plateaued thereafter. From these results, we determined the conditions for subsequent experiments, that is, the adsorption period of 24 h under shaking conditions.

3.5 Effect of bFGF concentration in the adsorption solution on the bFGF-release ability of the sheet

The amount of bFGF adsorbed onto the P10 sheet surface increased with increasing initial bFGF concentration in the bFGF solution. The P10 sheet was immersed for 24 h in the bFGF solutions with different concentrations ($x = 0$ – $12 \mu\text{g mL}^{-1}$) under shaking conditions (the resulting bFGF-adsorbed

P10 sheet is denoted as P10Fx). As shown in Fig. 5a, the amount of bFGF adsorbed onto the P10 sheet surface increased as the initial bFGF concentration in the bFGF solution increased from $0 \mu\text{g mL}^{-1}$ (P10F0) to $8 \mu\text{g mL}^{-1}$ (P10F8). We observed no significant difference in the amount of adsorbed bFGF between the P10F8 and P10F12 sheets. In the case of the P10F12 sheet, roughly 1/5 of the total bFGF added to the solution was adsorbed onto the sheet surface. Fig. 5b displays the same data plotted as a function of the equilibrated bFGF concentration in the solution after 24 h adsorption. This curve is the bFGF adsorption isotherm that can be explained by the Langmuir adsorption model. From this bFGF adsorption isotherm, we estimated the saturated adsorption amount of bFGF to be approximately $2.5 \mu\text{g}$ per sheet (*i.e.*, $2.5 \mu\text{g cm}^{-2}$).

The P10F8 and P10F12 sheets released bFGF into the acellular culture medium at a concentration close to or above the target level (10 ng mL^{-1}) for as long as 3 d. We performed the bFGF-release assay using the acellular culture medium for selected P10Fx sheets. As shown in Fig. 6, the bFGF-adsorbed P10 sheet exhibited different release profiles of bFGF in the acellular culture medium, depending on the initial bFGF concentration in the solution used in bFGF adsorption. Considering the results in Fig. 5a, the higher bFGF-release ability of the P10F8 and P10F12 sheets should be derived from the larger amount of bFGF adsorbed onto their surfaces. Although the difference in the bFGF-release ability between the P10F8 and P10F12 sheets was not significant, the P10F12 sheet released a higher average concentration of bFGF exceeding the target level (10 ng mL^{-1}) at all the assessed periods up to 3 d. Thus, we selected P10F12 as the optimal sheet and used it for subsequent cellular experiments.

3.6 bFGF-release ability of the sheet in the iPSC culture medium

The P10F12 sheet maintained the bFGF concentration above the target level (10 ng mL^{-1}) for 3 d in the culture medium of iPSCs.

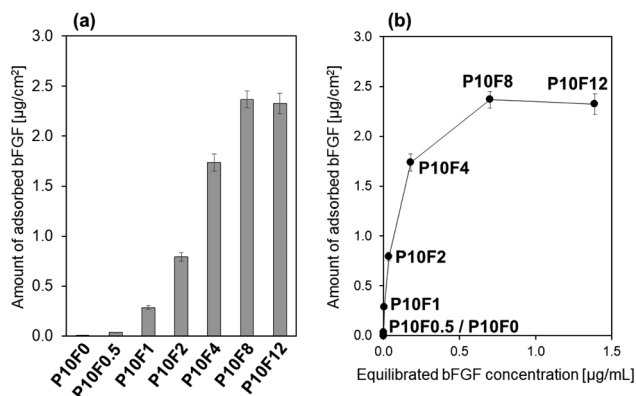


Fig. 5 (a) Amounts of bFGF adsorbed on the surfaces of the P10F0, P10F0.5, P10F1, P10F2, P10F4, P10F8, and P10F12 sheets and (b) those plotted as a function of the equilibrated bFGF concentration in the bFGF solution after adsorption for 24 h (average \pm SD; $n = 3$).

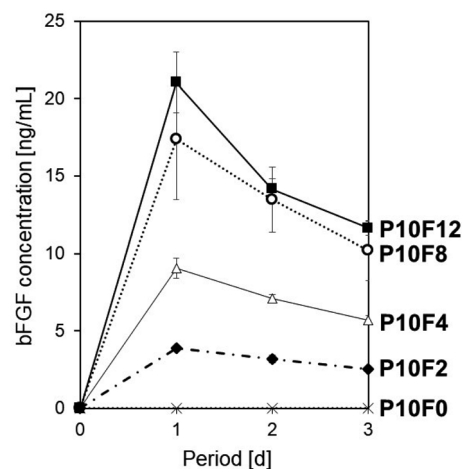


Fig. 6 Release profiles of bFGF in the acellular culture medium from the P10F0, P10F2, P10F4, P10F8, and P10F12 sheets (average \pm SD; $n = 3$).

The culture medium with precultured iPSCs and the acellular culture medium (the cell-free control) were supplemented with the P10F12 sheet. During medium-change-free continuous culture for 3 d, the bFGF concentration in the iPSCs-containing medium was higher than the target level (10 ng mL^{-1}) (see “Culture with sheet” in Fig. 7a). Without iPSCs in the medium, the bFGF concentration slightly decreased (see “Cell-free control” in Fig. 7a). Although we found a significant difference between these two profiles only at Day 2, the same tendency (*i.e.*, higher bFGF concentration in the presence of iPSCs) was reconfirmed by multiple independent experiments.

As a positive control, iPSCs were cultured under conventional conditions in the culture medium supplemented with 10 ng mL^{-1} of bFGF with daily medium change. The bFGF concentration in the medium at Days 1, 2, and 3, just before daily medium change, was as low as $1.3\text{--}1.4 \text{ ng mL}^{-1}$ (Fig. 7b). This result reconfirmed the quite low stability of bFGF at 37°C , as observed in the acellular culture medium (see “Free bFGF” in Fig. 3).

3.7 Effect of the sheet on colony formation and pluripotency of iPSC

The P10F12 sheet supported colony formation of iPSCs during medium-change-free continuous culture for 3 d, similarly to the positive control (conventional culture conditions). In the presence of the P10F12 sheet, the iPSCs proliferated to form large colonies with rounded edges at Day 3, even without medium change (upper images in Fig. 8). The observed colonies were apparently similar to normal colonies of iPSCs and those found in the positive control (middle images in Fig. 8). With neither the P10F12 sheet nor bFGF in the culture medium (negative control), the iPSCs formed smaller and dispersed colonies with jagged edges at Day 3 (lower images in Fig. 8), implying a certain change in cellular characteristics. We observed similar results for both Cultures 1 and 2.

Compared with the positive control, medium-change-free continuous culture with the P10F12 sheet had no significant effect on viability of the iPSCs, whereas it retarded cellular

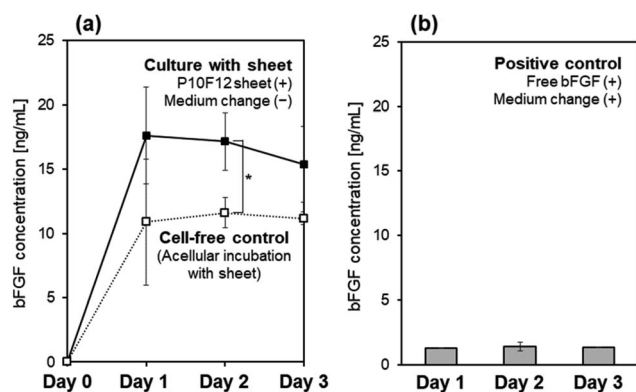


Fig. 7 (a) Release profiles of bFGF from the P10F12 sheet in the culture medium with and without iPSCs and (b) bFGF concentrations in the culture medium just before daily medium change at Days 1, 2, and 3 in the conventional culture of iPSCs with free bFGF (10 ng mL^{-1}) (positive control) in Culture 1 (average \pm SD; $n = 3$; $*p < 0.05$).

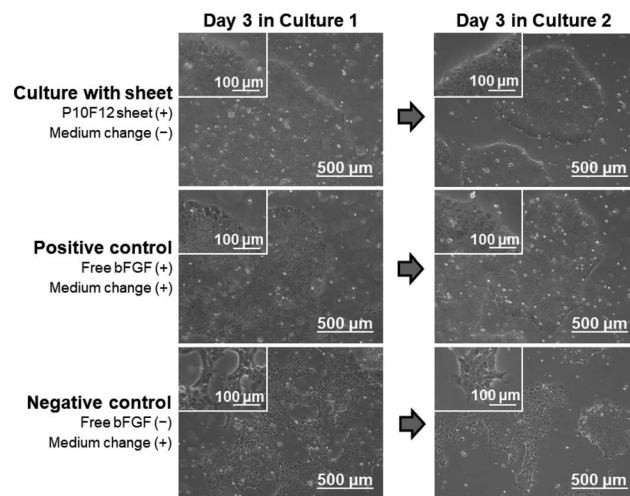


Fig. 8 Phase contrast microscopic images of iPSCs cultured with the P10F12 sheet without medium change (upper) or with (positive control; middle) and without (negative control; lower) free bFGF (10 ng mL^{-1}) with daily medium change at Day 3 in Culture 1 (left) and Culture 2 (right). Insets show higher magnification images.

proliferation. We assessed the number (per well) and viability (percentage of the viable cells) of the cultured iPSCs after Culture 1. The iPSCs cultured with the P10F12 sheet without medium change were fewer than those of the positive control (Fig. 9a), however, their viability was equivalent for both culture conditions (Fig. 9b).

The bFGF released from the P10F12 sheet retained its biological activity to preserve pluripotency of human iPSCs. The iPSCs after Culture 2 were assessed for pluripotency using three markers: rBC2LCN, Nanog, and Oct-3/4. Fig. 10 shows fluorescence images of the cultured iPSCs stained for rBC2LCN (left), Nanog (middle), and Oct-3/4 (right), and those counterstained with DAPI. The iPSCs cultured in the presence of the P10F12 sheet (upper 6 images in Fig. 10) exhibited signals of all three

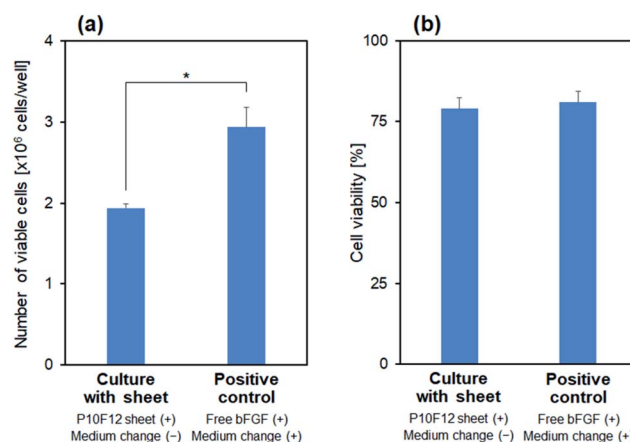


Fig. 9 (a) Number of viable iPSCs per well and (b) viability of iPSCs after Culture 1 with the P10F12 sheet without medium change or with free bFGF (10 ng mL^{-1}) with daily medium change (positive control) (average \pm SD; $n = 3$; $*p < 0.05$).

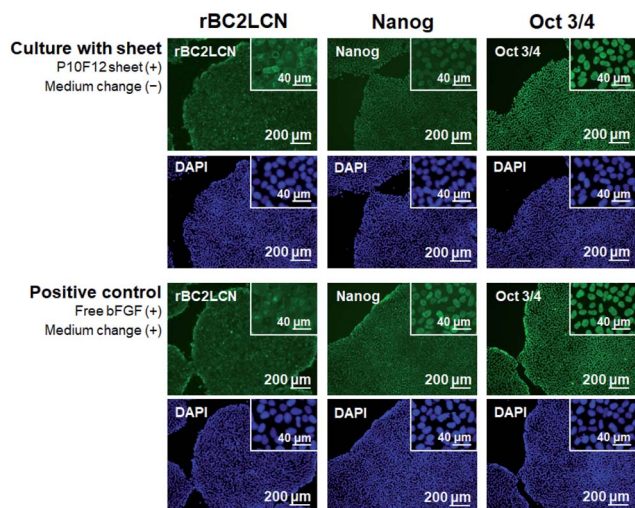


Fig. 10 Fluorescence microscopic images of iPSCs cultured with the P10F12 sheet without medium change (upper 2 rows) or with free bFGF (10 ng mL^{-1}) with daily medium change (positive control; lower 2 rows). The iPSCs were stained with FITC (green)-conjugated rBC2LCN (left), anti-Nanog (middle), and anti-Oct-3/4 (right) and their nucleus were counterstained with DAPI (blue) after Culture 2. Insets show higher magnification images.

pluripotency markers similarly to the iPSCs of the positive control (lower 6 images in Fig. 10). These results proved that iPSCs cultured in the presence of the P10F12 sheet retained their pluripotency even after medium-change-free continuous culture for 3 d.

We confirmed reproducibility of the results shown in Fig. 8–10 by multiple (2–4 times) independent experiments.

4 Discussion

4.1 Functions and advantages of the water-floatable PE nonwoven fabric sheet

We successfully prepared a bFGF-releasing water-floatable PE nonwoven fabric sheet by simple adsorption following oxygen plasma treatment. The prepared sheet (P10F12) allowed sustained release of bFGF into the culture medium and supported proliferation and colony formation of human iPSCs without deteriorating their pluripotency during medium-change-free continuous culture for 3 d. The thus-cultured iPSCs were apparently comparable to those cultured under the conventional conditions (positive control) in terms of colony morphology (Fig. 8), viability (Fig. 9b), and expression of pluripotency markers (Fig. 10). There was a difference in the number of proliferated viable iPSCs between two culture conditions; medium-change-free continuous culture for 3 d with the P10F12 sheet resulted in a smaller number of viable cells than the conventional culture (positive control) (Fig. 9a). This result suggests the retarded proliferation rate under the former culture conditions. This might be caused by the reduction of other nutrients besides bFGF and/or accumulation of cellular debris and wastes in the medium during medium-change-free continuous culture.

The bFGF-releasing water-floatable PE nonwoven fabric prepared in this study has potential as a new form of bFGF supplement for culture media of human stem cells. It has several advantages in its formulation over matrix-based bFGF-releasing materials. First, the sheet comprises chemically stable PE, and its bFGF release is not mediated by matrix degradation but by desorption from its surface. Second, the sheet immobilizes bFGF on its surface without the aid of any bFGF-binding agents, such as heparin³⁶ or fibrinogen.^{37,38} Thus, the sheet can supply bFGF to the culture medium without contaminating it with either matrix degradation products or bFGF-binding agents. After use, the sheet can be easily taken out and completely separated from the cells, leaving no residue in the culture medium. Moreover, the sheet floats in the culture medium and secures a certain distance from the cells so as not to physically come in contact with the cell surfaces even without the aid of culture plate inserts. Given these features, the sheet itself is considered to have minimal biological and physical effects on stem cells.

4.2 Effects of oxygen plasma treatment on bFGF adsorption

To immobilize a sufficient amount of bFGF by simple bFGF adsorption, we employed a PE nonwoven fabric sheet with a large surface area and modified its surface with polar functional groups by oxygen plasma treatment (Fig. 2a). On the plasma-treated sheet surface, oxygen-containing polar functional groups, such as OH, COOH, and CHO, formed through the cleavage of ethylene linkages in PE and reactions with active species from the oxygen plasma.^{33,34,39} The plasma-treated sheet certainly adsorbed a larger amount of bFGF onto its surface than the untreated sheet (Fig. 2b). This can be explained by chemical and physical factors as detailed next.

The chemical factor is the increased surface affinity of the plasma-treated sheet with bFGF. The plasma-treated PE surface possesses higher interfacial free energy and, thus, a greater thermodynamic driving force for bFGF adsorption than the untreated PE surface. In addition, the plasma-treated PE surface has greater attractive electric force for bFGF than the untreated PE surface. This is because oxygen plasma treatment increases the negative surface charge of PE,³⁴ whereas the basic protein bFGF is positively charged in neutral solutions.

The physical factor is the enhanced diffusion of the bFGF solution within the plasma-treated nonwoven fabric sheet, which increases the number of adsorption sites by enlarging the area of solid–liquid interface. Previous studies have reported that plasma treatment increases water wettability of a polymer fabric, thereby increasing the rate and depth of diffusion of an aqueous dye into the fabric *via* capillary action.^{40,41} Such a phenomenon was observed for the P10 sheet used in this study, as depicted in Fig. 1c. The P10 sheet with the hydrophilic and water-wetting surface allowed prompt diffusion of the solution within it so that the P10 sheet was completely submerged in the solution upon contact with it. Conversely, the P00 sheet with the hydrophobic and water-repulsive surface inhibited the solution from diffusing within it.

Although the prior plasma treatment was essential to obtain a bFGF-releasing nonwoven fabric sheet, its bFGF-release ability

was hardly affected by the plasma power density under the tested conditions from 0.5 to 2.0 W cm⁻² (Fig. 3). This might be because all the plasma-treated sheets (P05, P10, and P20) had a similar water wettability (Fig. 1b).

4.3 Effects of shaking on bFGF adsorption

Shaking of the bFGF solution accelerated adsorption of bFGF onto the P10 sheet (Fig. 4). This result implies that bFGF adsorption onto the P10 sheet is diffusion limited. Although the P10 sheet was submerged in the bFGF solution instantly upon contact with it, bFGF adsorption onto the P10 sheet progressed slowly with time. As shown in Fig. 4b, the adsorption period required to reach equilibrium was as long as 24 h even under shaking conditions. Such long-lasting adsorption is attributed to the restricted diffusion within the P10 sheet and is typical of nonwoven fabrics with an interconnected nanoporous structure.

4.4 Desorption and release of bFGF

The P10F12 sheet prepared under optimum conditions desorbed bFGF from its surface and successfully maintained the bFGF concentration in the culture medium to ≥ 10 ng mL⁻¹ for 3 d (Fig. 6 and 7a). bFGF desorption from the P10F12 sheet might be due to the altered equilibrium in the medium that has a much lower bFGF concentration (zero at the starting point) and higher temperature (37 °C) than the bFGF solution (12 μ g mL⁻¹, 25 °C) used in bFGF adsorption (phenomenon known as Le Chatelier's principle). Exchange reactions between bFGF molecules adsorbed onto the P10F12 sheet and other biomolecules (transferrin, insulin, *etc.*) contained in the medium might also be involved in bFGF desorption from the P10F12 sheet. Such exchange reactions may potentially reduce the concentrations of other biomolecules in the medium, although such an effect was not examined in this study.

As shown in Fig. 7b, free bFGF (10 ng mL⁻¹) added to the culture medium dramatically reduced (1/8–1/7 of the initial concentration) within 24 h. On the other hand, in the medium supplemented with the P10F12 sheet, the bFGF concentration did not decrease but remained at a similar level for up to 3 d (Fig. 7a). These results indicate that the P10F12 sheet continuously supplied bFGF to the medium *via* sustained release of bFGF. This could be attributed to the restricted diffusion within the interconnected nanoporous structure of the P10F12 sheet. Interestingly, the bFGF concentration in the medium was significantly increased by the presence of iPSCs at Day 2 (compare two profiles in Fig. 7a). Although the detailed mechanism remains to be elucidated, we believe that the secretion of bFGF and/or bFGF-stabilizing agents (such as heparin) by iPSCs themselves might be related to this phenomenon. Secretion of other biomolecules (cytokines, extracellular matrix components, *etc.*) by iPSCs may also increase the bFGF concentration in the medium by enhancing bFGF desorption from the sheet *via* exchange reactions or reducing nonspecific bFGF adsorption onto the wells' inner wall.

An overdose of bFGF in a culture medium has an adverse effect on stem cell maintenance. For example, proliferation and colony formation of human embryonic stem cells were enhanced with increasing bFGF concentration in a medium (hESF8

medium, heparin(-)) up to 50 ng mL; however, at 100 ng mL⁻¹ bFGF, colony sizes became smaller and apparently differentiated cells appeared.¹⁰ With the P10F12 sheet, the bFGF concentration in the iPSC-containing culture medium ranged from approximately 15 to 18 ng mL⁻¹ (Fig. 7a), which was slightly higher than the target level (10 ng mL⁻¹). Thus, it might be possible to decrease bFGF concentration in the adsorption solution from 12 μ g mL⁻¹ (for P10F12) to 8 μ g mL⁻¹ (for P10F8) or even lower, enabling reduction of bFGF usage as well as the overdose risk. Further studies are needed to verify this hypothesis.

4.5 Perspectives

In this study, we prepared a bFGF-releasing water-floatable PE nonwoven fabric sheet for use as a bFGF supplement for stem cell maintenance. In addition to the effect on stem cell maintenance, bFGF has several other biological effects, for example, an accelerating effect on angiogenesis and regeneration of dermal, nervous, bone, and periodontal tissues.^{1–6} For other applications besides stem cell maintenance, other fabric sheets made of different polymers can be used as a bFGF adsorbent. Nonwoven fabric sheets are considered capable of immobilizing not only bFGF but also other cytokines with different biological effects *via* the same approach, *i.e.*, plasma-induced surface modification followed by cytokine adsorption. The biological effects of cytokines are generally dose-dependent; thus local dose control at the site of action is an important factor for achieving desired results *in vitro* and *in vivo*. This study demonstrated that the bFGF content and bFGF-release profile of the fabric sheet are controllable to a certain extent by tuning the bFGF adsorption conditions (*i.e.*, adsorption time, shaking/static conditions, and bFGF concentration in the adsorption solution). Thus, the results offer a design guide for fabric sheets with tailored cytokine-release profile that would be potentially useful in a wide variety of biomedical applications.

Subjects of future studies include elucidation of bFGF adsorption/desorption mechanisms, further process refinement to improve cell proliferation rate and to improve bFGF immobilization efficiency (to reduce bFGF usage), efficacy validation after long-term culture (after a number of passages), assessment of storage stability, application to other cytokines besides bFGF, and exploration of other biomedical applications.

5 Conclusions

Water-floatable PE nonwoven fabric sheets with bFGF-releasing ability were prepared by simple adsorption following oxygen plasma treatment. The P10F12 sheet prepared under optimized conditions released bFGF in a sustained manner and maintained the bFGF concentration in the culture medium of human iPSCs at ≥ 10 ng mL⁻¹ during medium-change-free continuous culture for 3 d. The bFGF released from the P10F12 sheet retained its biological activity to support colony formation of iPSCs while preserving their pluripotency. This type of bFGF-releasing sheet would be a new form of bFGF supplement for culture media of stem cells and make a significant contribution to stem cell-based research and development.

Conflicts of interest

This work was supported in part by Japan Science and Technology Agency (JST) Matching Planner Program and in part by Katayama Chemical Industries Co., Ltd., Japan. The nonwoven fabric sheet and bFGF were supplied by DuPont-Asahi Flash Spun Products Co., Ltd., Japan and Katayama Chemical Industries Co., Ltd., Japan, respectively.

Acknowledgements

We appreciate Ms Ikuko Sakamaki from AIST for technical support, Dr Keiichi Ikegami from AIST and Dr Takayuki Otani from Katayama Chemical Industries Co., Ltd. for scientific advice, and Mr Teruhisa Otsuka from AIST for XPS measurements. XPS measurements were conducted at AIST Nano-Processing Facility supported by “Nanotechnology Platform” of the Ministry of Education, Culture, Sports, Science and Technology (MEXT), Japan. This work was supported in part by Japan Science and Technology Agency (JST) Matching Planner Program and in part by Katayama Chemical Industries Co., Ltd., Japan.

References

- 1 L. Maddaluno, C. Urwyler and S. Werner, *Development*, 2017, **144**, 4047.
- 2 J. Slavin, *Cell Biol. Int.*, 1995, **19**, 431.
- 3 M. Allouche, *Leukemia*, 1995, **9**, 937.
- 4 J. S. Wang, *Acta Orthop. Scand.*, 1996, **67**, 1.
- 5 S. Murakami, *Periodontol. 2000*, 2011, **56**, 188.
- 6 C. Grothe and G. Nikkha, *Anat. Embryol.*, 2001, **204**, 171.
- 7 M. Amit, M. K. Carpenter, M. S. Inokuma, C. P. Chiu, C. P. Harris, M. A. Waknitz, J. Itskovitz-Eldor and J. A. Thomson, *Dev. Biol.*, 2000, **227**, 271.
- 8 R. H. Xu, R. M. Peck, D. S. Li, X. Feng, T. Ludwig and J. A. Thomson, *Nat. Methods*, 2005, **2**, 185.
- 9 M. Kinehara, S. Kawamura, D. Tateyama, M. Suga, H. Matsumura, S. Mimura, N. Hirayama, M. Hirata, K. Uchio-Yamada, A. Kohara, K. Yanagihara and M. K. Furue, *PLoS One*, 2013, **8**, e54122.
- 10 M. K. Furue, J. Na, J. P. Jackson, T. Okamoto, M. Jones, D. Baker, R.-I. Hata, H. D. Moore, J. D. Sato and P. W. Andrews, *Proc. Natl. Acad. Sci. U. S. A.*, 2008, **105**, 13409.
- 11 M. Ohnuki, K. Takahashi and S. Yamanaka, *Curr. Protoc. Stem Cell Biol.*, 2009, **9**, 4A.2.–1.
- 12 G. Chen, D. R. Gulbranson, P. Yu, Z. Hou and J. A. Thomson, *Stem Cells*, 2012, **30**, 623.
- 13 M. E. Levenstein, T. E. Ludwig, R.-H. Xu, R. A. Llanas, K. VanDenHeuvel-Kramer, D. Manning and J. A. Thomson, *Stem Cells*, 2006, **24**, 568.
- 14 S. Lotz, S. Goderie, N. Tokas, S. E. Hirsch, F. Ahmad, B. Corneo, S. Le, A. Banerjee, R. S. Kane, J. H. Stern, S. Temple and C. A. Fasano, *PLoS One*, 2013, **8**, e56289.
- 15 U. Han, H. H. Park, Y. J. Kim, T. H. Park, J. H. Park and J. Hong, *ACS Appl. Mater. Interfaces*, 2017, **9**, 25087.
- 16 G. Zhu, S. R. Mallery and S. P. Schwendeman, *Nat. Biotechnol.*, 2000, **18**, 52.
- 17 K. E. Park, B. S. Kim, M. H. Kim, H. K. You, J. Lee and W. H. Park, *Polymer*, 2015, **76**, 8.
- 18 J. Zhu, *Biomaterials*, 2010, **31**, 4639.
- 19 S. Cai, Y. Liu, X. Z. Shu and G. D. Prestwich, *Biomaterials*, 2005, **26**, 6054.
- 20 M. Tanihara, Y. Suzuki, E. Yamamoto, A. Noguchi and Y. Mizushima, *J. Biomed. Mater. Res.*, 2001, **56**, 216.
- 21 Y. Tabata and Y. Ikada, *Adv. Drug Delivery Rev.*, 1998, **31**, 287.
- 22 S. E. Sakiyama-Elbert and J. A. Hubbell, *J. Controlled Release*, 2000, **65**, 389.
- 23 M. Matsusaki and M. Akashi, *Biomacromolecules*, 2005, **6**, 3351.
- 24 H. Mori, C. Shukunami, A. Furuyama, H. Notsu, Y. Nishizaki and Y. Hiraki, *J. Biol. Chem.*, 2007, **282**, 17289.
- 25 Y. Sogo, A. Ito, M. Onoguchi, A. Oyane, H. Tsurushima and N. Ichinose, *Biomed. Nanomater.*, 2007, **2**, S175.
- 26 H. Tsurushima, A. Marushima, K. Suzuki, A. Oyane, Y. Sogo, K. Nakamura, A. Matsumura and A. Ito, *Acta Biomater.*, 2010, **6**, 2751.
- 27 Y. Yazaki, A. Oyane, Y. Sogo, A. Ito, A. Yamazaki and H. Tsurushima, *Biomaterials*, 2011, **32**, 4896.
- 28 G. Chen, D. R. Gulbranson, Z. Hou, J. M. Bolin, V. Ruotti, M. D. Probasco, K. Smuga-Otto, S. E. Howden, N. R. Diol, N. E. Propson, R. Wagner, G. O. Lee, J. Antosiewicz-Bourget, J. M. C. Teng and J. A. Thomson, *Nat. Methods*, 2011, **8**, 424.
- 29 K. Takahashi, K. Tanabe, M. Ohnuki, M. Narita, T. Ichisaka, K. Tomoda and S. Yamanaka, *Cell*, 2007, **131**, 861.
- 30 Y. Onuma, K. Higuchi, Y. Aiki, Y. Shu, M. Asada, M. Asashima, M. Suzuki, T. Imamura and Y. Ito, *PLoS One*, 2015, **10**, e0118931.
- 31 Y. Onuma, H. Tateno, J. Hirabayashi, Y. Ito and M. Asashima, *Biochem. Biophys. Res. Commun.*, 2013, **431**, 524.
- 32 A. Vesel, *Inf. MIDEM*, 2008, **38**, 257.
- 33 S. Guruvenket, G. M. Rao, M. Komath and A. M. Raichur, *Appl. Surf. Sci.*, 2004, **236**, 278.
- 34 M. Lehocný, H. Drnovská, B. Lapčíková, A. M. Barros-Timmons, T. Trindade, M. Zembala and L. Lapčík Jr, *Colloids Surf., A*, 2003, **222**, 125.
- 35 M. J. Davies, C. A. Mitchell, M. A. L. Maley, M. D. Grounds, A. R. Harvey, G. W. Plant, D. J. Wood, Y. Hong and T. V. Chirila, *J. Biomater. Appl.*, 1997, **12**, 31.
- 36 J. T. Gallagher and J. E. Turnbull, *Glycobiology*, 1992, **2**, 523.
- 37 M. M. Martino, P. S. Briquez, A. Ranga, M. P. Lutolf and J. A. Hubbell, *Proc. Natl. Acad. Sci. U. S. A.*, 2013, **110**, 4563.
- 38 A. Sahni, T. Odriljin and C. W. Francis, *J. Biol. Chem.*, 1998, **273**, 7554.
- 39 F. D. Egitto and L. J. Matienzo, *IBM J. Res. Dev.*, 1994, **38**, 423.
- 40 A. E. A. Elabid, J. Zhang, J. Shi, Y. Guo, K. Ding and J. Zhang, *Appl. Surf. Sci.*, 2016, **375**, 26.
- 41 A. Raffaele-Addamo, E. Selli, R. Barni, C. Riccardi, F. Orsini, G. Poletti, L. Meda, M. R. Massafra and B. Marcandalli, *Appl. Surf. Sci.*, 2016, **252**, 2265.